Errors in Acoustic Doppler Profiler Velocity Measurements Caused by Flow Disturbance

David S. Mueller[1]; Jorge D. Abad[2]; Carlos M. García[3]; Jeffery W. Gartner[4]; Marcelo H. García[5]; and Kevin A. Oberg[6]

Abstract: Acoustic Doppler current profilers (ADCPs) are commonly used to measure streamflow and water velocities in rivers and streams. This paper presents laboratory, field, and numerical model evidence of errors in ADCP measurements caused by flow disturbance. A state-of-the-art three-dimensional computational fluid dynamic model is validated with and used to complement field and laboratory observations of flow disturbance and its effect on measured velocities. Results show that near the instrument, flow velocities measured by the ADCP are neither the undisturbed stream velocity nor the velocity of the flow field around the ADCP. The velocities measured by the ADCP are biased low due to the downward flow near the upstream face of the ADCP and upward recovering flow in the path of downstream transducer, which violate the flow homogeneity assumption used to transform beam velocities into Cartesian velocity components. The magnitude of the bias is dependent on the deployment configuration, the diameter of the instrument, and the approach velocity, and was observed to range from more than 25% at 5 cm from the transducers to less than 1% at about 50 cm from the transducers for the scenarios simulated.

DOI: 10.1061/(ASCE)0733-9429(2007)133:12(1411)

CE Database subject headings: Flow measurement; Acoustic techniques; Computational fluid dynamics technique; Numerical models; Errors; Velocity.

Introduction

The use of acoustic Doppler current profilers (ADCPs) for making discharge and water velocity measurements in streams and rivers has increased dramatically as manufacturers have refined the acoustic technique for use in depths as shallow as 0.6 m (Oberg and Mueller 1994; Simpson 2002; Oberg et al. 2005). About 20% of the discharge measurements made by the U.S. Geological Survey in water year 1990 (October 1, 1989–September 30, 1990) were made in streams with a mean depth between 0.38 and 0.61 m (Fulford 1992). In addition, the ADCP has become the tool of choice for mapping velocity fields that are used to assess aquatic habitat and validate numerical models (Jacobson et al. 2004; Wagner and Mueller 2001). The blanking distance from the transducers required before valid data can be obtained is one of the issues limiting the minimum depth for ADCP measurements. Blanking distance is the distance (time) the emitted sound travels while internal electronics prepare for data reception and the transducers stop vibrating from the transmission and become quiescent enough to accurately record the backscattered acoustic energy. The typical minimum blanking distance for general purpose ADCPs has been 20–25 cm. Recent transducer developments have reduced this blanking distance to as little as 5 cm. However, the disturbance effects of the flow field developed around the ADCP on measurements near the transducer have not been previously considered.

This paper presents laboratory data, field data, and numerical simulations to show that errors in acoustic Doppler velocity measurements can be caused by instrument-induced flow disturbance. The modeling approach is introduced and the main characteristics of the computational fluid dynamic (CFD) model used in the analysis are summarized. The CFD model is validated using benchmark experiments from other studies and particle image velocimeter (PIV) velocity measurements in a laboratory experiment under nonfully developed turbulent flow conditions. CFD simulations that duplicate the field data reported by Gartner and Ganju (2002) provide hydrodynamic evidence that near-instrument flow velocities measured by the ADCP are neither the undisturbed stream velocity nor the velocity of the flow field around the ADCP. Finally, CFD simulations are used to evaluate effect of different flow conditions (different Froude and Reynolds numbers) on actual velocity patterns and the velocity

[1]Hydrologist, Office of Surface Water, U.S. Geological Survey, 9818 Bluegrass Pkwy., Louisville, KY 40299. E-mail: dmueller@usgs.gov

[2]Graduate Student, Ven Te Chow Hydrosystems Laboratory, Univ. of Illinois, 205 N. Mathews, Urbana, IL 61801. E-mail: abad@uiuc.edu

[3]Professor, Instituto Superior de Recursos Hídricos, Universidad Nacional de Córdoba. Av. Filloy s/n. Ciudad Universitaria, Córdoba, Argentina. E-mail: cgarcia2mjc@gmail.com

[4]Oceanographer, National Research Program, U.S. Geological Survey, 520 N. Park Ave., Tucson, AZ 85719. E-mail: jgartner@usgs.gov

[5]Chester and Helen Siess Professor, and Director, Ven Te Chow Hydrosystems Laboratory, Dept. of Civil and Environmental Engineering, Univ. of Illinois at Urbana-Champaign, 205 North Mathews Ave., Urbana, IL 61801. E-mail: mhgarcia@uiuc.edu

[6]Hydrologist, Office of Surface Water, U.S. Geological Survey, 1201 W. University Ave., Ste. 100, Urbana, IL 61801-2748. E-mail: kaoberg@usgs.gov

Note. Discussion open until May 1, 2008. Separate discussions must be submitted for individual papers. To extend the closing date by one month, a written request must be filed with the ASCE Managing Editor. The manuscript for this paper was submitted for review and possible publication on April 20, 2006; approved on August 7, 2007. This paper is part of the ***Journal of Hydraulic Engineering***, Vol. 133, No. 12, December 1, 2007. ©ASCE, ISSN 0733-9429/2007/12-1411–1420/$25.00.

profile the ADCP would have measured from the simulated flow field.

Errors Observed in ADCP Field Measurements

Gartner and Ganju (2002) observed distortion in velocity profiles measured by a stationary downward-looking Teledyne RD Instruments Rio Grande ADCP (Note: Any use of trade, product, or firm names is for descriptive purposes only and does not imply endorsement by the U.S. Government) in the San Joaquin River at Vernalis, California, and the Delta Mendota Canal at Byron, California. Initial tests in the San Joaquin River at Vernalis, California showed velocity magnitudes measured by ADCP in the upper three or four bins were less than those measured by a SonTek/YSI acoustic Doppler velocimeter (ADV) mounted near the ADCP. The bins closest to the transducer had the largest negative bias (10% to 15%). Subsequent measurements were made on the Delta Mendota Canal at Bryon, California to evaluate the effect of varying the blanking distance (between 5 and 25 cm) on the measured velocity profile. The Delta Mendota Canal is a man-made concrete (trapezoidal) channel approximately 30 m wide at surface and about 5 m deep. During the tests, the water speed was nearly constant (+/− about 1.5%) through the range of depths (about 30–130 cm) sampled by the ADV. ADCP- and ADV-measured velocities compared favorably below about 70 cm from the water surface, indicating that the difference in sample volumes between instruments had a negligible effect on the observed biases. Although the aspect ratio of the channel was 5:1, no evidence suggesting secondary circulation that would cause maximum velocities below surface was found within 130 cm of surface. The 1,200 kHz ADCP was configured for water mode 5, 5 cm bins, and an immersion depth of 21.5 cm. The use of water mode 5 in this depth of water with a 1,200 kHz ADCP resulted in only the top half of the velocity profile being measured. ADCP (single ping) measurements spanned at least 205 s to correspond with the ADV samples. For each set of measurements, the ADV was positioned on a bridge across the canal in the middle of a long and straight section about 1.5 m from the ADCP and at a depth corresponding to the center of bin 1 of the ADCP. The ADV was programmed to sample at 10 Hz using 100 cm/s velocity scale for 2,048 samples. Similar to previous results at Vernalis, portions of velocity profiles near surface were biased low (Fig. 1).

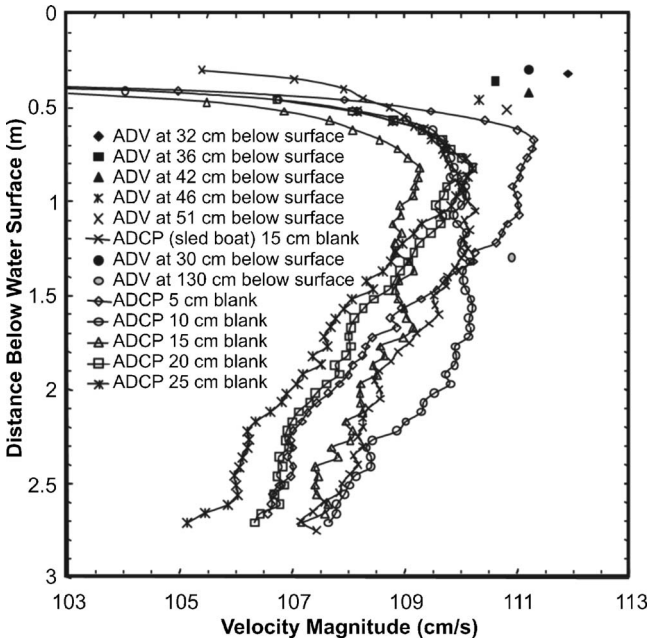

Fig. 1. ADCP velocity profiles and ADV point velocity measurements in Delta Mendota Canal at Bryon, Calif., on January 24, 2002

Approach

Velocities measured by an ADCP in Cartesian coordinates are based on the assumption that flow is homogeneous in all of the beams. The Doppler shift is a vector quantity and ADCPs can only measure velocities parallel to the acoustic beams. Velocities with Cartesian coordinates are determined by assuming flow homogeneity between the beams and applying appropriate trigonometric transformations (RD Instruments 1999; SonTek 2000). If the flow is heterogeneous (flow is not the same in each beam because of flow disturbances), the trigonometric transformations are not valid and will result in an incorrect Cartesian velocity. The hypothesis presented herein is that measurement of velocities by an ADCP too close to the instrument not only violates the flow homogeneity assumption, but also produces velocity magnitudes that are contrary to expected velocities near a flow obstruction. As flow is diverted under and around an ADCP, the velocities increase near the ADCP. However, the ADCP-measured velocities in the vicinity of the instrument are less than the undisturbed velocities. The hypothesis is best illustrated by considering the fore and aft beams of a four-beam system aligned with the flow. The flow deflected by the ADCP is downward in the upstream beam and upward to flat in the downstream beam. When the measured beam velocities are resolved to a two-dimensional velocity, the result is a velocity of lower magnitude. Thus, the velocity measured by the ADCP is neither the undisturbed stream velocity nor the velocity of the flow around the ADCP.

Other possible causes for the observed velocity bias besides the shape of the flow field caused by the instrument have been evaluated and subsequently discounted. Gartner and Ganju (2002) discussed the potential for decorrelation in pulse coherent modes caused by flow acceleration as the water moved around the instrument. Data collected using other modes showed the same tendency, suggesting that decorrelation was not the cause of the distortion. Residual of the transmitted acoustic signal (ringing) present during velocity measurements will cause the measured velocity to be low because there is a zero Doppler shift in the residual of the transmitted signal. Evaluation of the instrument used by Gartner and Ganju (2002) and other similar instruments show little or no ringing beyond 5–10 cm from the transducers. Thus, ringing was not the primary cause of the bias observed by Gartner and Ganju (2002). Ping-to-ping interference can occur when a ping (acoustic pulse) transmitted by the ADCP has not dissipated sufficiently before another ping is transmitted. The residual acoustic energy from the earlier ping is typically energy reflected from the streambed or nearby obstruction, which would contain a Doppler shift near zero. Correspondingly, ping-to-ping interference will typically cause a low bias in measured velocities. The depth and water conditions observed by Gartner and Ganju (2002) were such that ping-to-ping interference was unlikely.

Since it was determined that other potential causes were not responsible for the velocity bias observed by Gartner and Ganju (2002), a detailed analysis of the effect of the flow disturbance by

the instrument on the measured velocities was undertaken to better understand the cause, magnitude, and spatial extent of the bias for a range of conditions. The observed bias could be affected by the shape, draft, and deployment mechanism of the ADCP in addition to the complex hydrodynamics of natural streams and rivers. A purely field-based approach to evaluating this bias would not be efficient nor allow the control of various important variables (velocity, depth, boundary roughness, and shape of deployment platforms). Laboratory-based approaches simplify the problem by allowing control of some variables associated with complex field conditions; however, due to limitations on measurement techniques, instrumentation, and flume size, the complete spectrum of possibilities cannot be studied. A numerical-model based approach that utilized both field and laboratory data to validate the suitability and accuracy of the numerical model was adopted to allow investigation of different depths, velocities, boundary roughness, and deployment configurations.

Numerical Model

Flow around an ADCP is characterized by free-surface distortion, a three-dimensional separation of the flow around the sides and bottom of the instrument, and a wake region behind the instrument. Numerically modeling the flow around an ADCP requires that the model be able to represent the instrument and deployment configuration accurately, while modeling the key features of the flow field accurately and efficiently. The model should provide the capability for a custom and (or) logarithmic velocity boundary condition at the upstream boundary and the capability to transport flow out of the downstream boundary with minimal upstream disturbance from the boundary. Additionally, the importance of modeling the free surface and the use of an appropriate turbulence closure model were carefully considered.

Model Characteristics

ADCPs are commonly used near the water surface and require some mechanism to deploy the instrument. The ADCP and its deployment configuration are flow obstructions that affect flow dynamics along the water column. The effect of free-surface distortion on the water column caused by the ADCP and (or) deployment configuration should be taken into consideration in the CFD model. A model utilizing an Eulerian interface capturing technique, known as the volume of fluid (VOF) (Hirt and Nichols 1981), was used. The VOF technique has been widely used for engineering purposes where free-surface modeling is of major concern (Richardson and Panchang 1996; Savage and Johnson 2001). The issue of the proximity of obstacles near the free surface was widely studied for the case of horizontal cylinders (Sheridan et al. 1997). Recently, Reichl et al. (2005) used a CFD model (FLUENT, Fluent Incorporated, Lebanon, N.H.) to model the flow pattern around submerged horizontal cylinders, and they highlighted the necessity of using an interface (air-water) capturing technique for attaining reliable results. Therefore, a state-of-the-art commercial model, FLOW-3D version 9.0 (Flow Science 2005), was used to analyze the flow pattern around the ADCP.

It is well known that the flow behind obstacles produces vortex shedding (e.g., Roulund et al. 2005; Johnson and Ting 2003). This type of phenomena is known as the "periodic flow phenomena" (Eberhard and Wille 1972). The use of large eddy simulation (LES) is beneficial in cases where large-scale unsteady motions are present (Pope 2004); however, LES models are still under development (Pope 2004; Iliescu and Fischer 2003; Meneveau and Katz 2000) and the application of LES for engineering purposes is limited, due to the dependence of the results on the configuration of the computational mesh. This limitation prevents direct extrapolation of laboratory-scale modeling to field-scale modeling. LES models also require very fine meshes to resolve the different scales on the turbulence spectrum (having very small time-steps), which makes LES simulations computationally expensive. Therefore, since our objective is the application of the CFD model to different scenarios (hydraulic conditions), an engineering-type turbulence closure is used. Some features and characteristics of periodic phenomena cannot be completely simulated by standard k-ε turbulence models (Younis and Przulj 2005). The renormalized group turbulence model (Yakhot and Nakayama 1986; Yakhot and Smith 1992; Shyy et al. 1997) is used based on its ability to predict the vortex shedding appropriately (Younis and Przulj 2005). Additional information on the application of FLOW-3D to this class of problem is provided in Abad et al. (2004).

Model Validation with Experimental Data

The validation of the CFD model was achieved by modeling benchmark experimental results, and detailed PIV laboratory measurements of flow around an ADCP deployed in a flume. Several benchmark experimental results associated with flow around solid obstacles have been reported in the literature. Reichl et al. (2005) showed that VOF could be used to appropriately model the free-surface deformation caused by infinite submerged horizontal cylinders close to the free surface (Sheridan et al. 1997; Hoyt and Sellin 2000) for different Froude and Reynolds numbers. Flow around bridge piers, pipelines, and weirs are common situations encountered by hydraulic engineers. Ahmed and Rajaratnam (1998) presented laboratory measurements of flow around piers and Barbhuiya and Dey (2004) presented measurements of flow around a vertical semicircular cylinder attached to the sidewall in a rectangular open channel flow. These two previous experiments were modeled and the results of the FLOW-3D model compared favorably with the published observations (comparison not presented herein).

Description of Laboratory Experiments

The flow disturbance caused by a SonTek/YSI acoustic Doppler profiler (ADP) was studied experimentally in an open channel flume $4.5 \times 0.40 \times 0.30$ m in length, width and height (x, y, and z, with $x=0$ at upstream end, $y=0$ in center of flume, and $z=0$ at bed of flume), respectively. The combination of length of the channel and desired water depth did not provide a fully developed turbulent flow. PIV was used to measure detailed two-dimensional (2D) velocities along the centerline of the flume, 2.3 m from the entrance of the flume (Fig. 2), with and without the presence of the ADP. Only the flow disturbance caused by the ADP could be evaluated because the depth of flow was too shallow for the ADP to measure the flow. A 120 mJ double-pulsed neodymium-doped yttrium aluminum garnet (Nd:YAG) laser was used to illuminate (through the transparent bottom of the flume) a region of the flow field in the center line of the flume. This configuration allowed collection of a complete representation of the flow field around the ADP without shadow areas. Image pairs were captured with a 4000 μs interval using a PIVCAM 40–15 Powerview 2000 by 2000 pixel digital camera. The camera had a 50 mm lens and was synchronized with the laser. The size of the capture field was

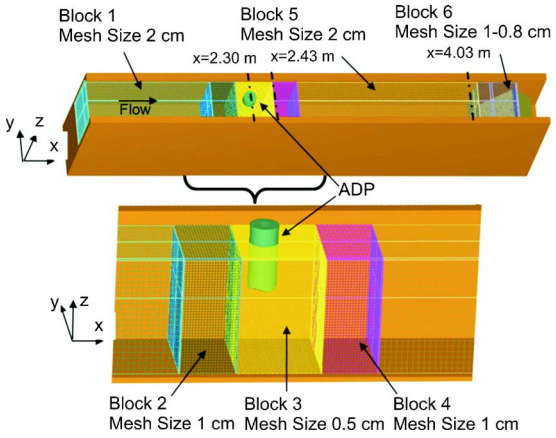

Fig. 2. Illustration of the computational meshes for CFD simulation of laboratory experiments on flow around the ADP

33.6 cm by 33.6 cm and a 5 Hz sampling frequency was used in this analysis. Seeding particles were added to the flow to improve the quality of the captured images. At the centerline of the flume, 2.3 m from the entrance, the water depth, mean velocity, hydraulic radius, and Reynolds number were 0.32 m, 0.143 m/s, 0.103 m, and 14,596, respectively. The deepest part of the instrument was located 23 cm from the bottom, which resulted in an 8 cm immersion depth (to center of transducers). Because the measurements were collected at different times (with and without the ADP), the time series of image pairs needed to be long enough to reduce the uncertainty in the statistical estimator of the mean and variance of the flow velocity signals for each of the three Cartesian components. Based on preliminary tests, 1,000 image pairs were used to minimize the effect of sampling the flow field at different times.

Simulation of Laboratory Experiments

A Cartesian computational mesh was prepared using a multiblock technique (Barkhudarov 2004) with six linked blocks. These blocks were arranged to use a coarse mesh throughout the majority of the flume, but provide a finer resolution to accurately represent the ADP and tailgate geometry using the fractional area/volume obstacle representation (FAVOR) method, without exceeding a 2:1 size ratio between adjacent cells in any of the three axes (Fig. 2). The computational cell sizes are 2, 1, 0.5, 1, 2, and 1 to 0.8 cm for blocks 1 through 6, respectively.

The flume had a nonuniform velocity and turbulent kinetic energy (TKE) distribution at the entrance that was not measured with sufficient resolution to allow direct use of the measured condition as the upstream boundary for the CFD model. The flume was also observed to have a meandering current that also was not well captured in the data collected. Therefore, CFD model boundary was positioned 1 m from the flume entrance and the velocity and TKE magnitude and distributions were adjusted to achieve good agreement with the observed data with no ADP in the flume. A continuative boundary condition (zero normal derivatives at the boundary for all quantities) was used at the exit to simulate a smooth continuation of the flow through the boundary. Wall boundary conditions were used along the sides of the flume. The top boundary was a free surface, modeled using VOF. Comparisons of the streamwise ADV- and PIV-measured velocities were made at three lateral locations ($y=-0.076$, 0, and 0.086 m) at two different streamwise locations ($x=2.43$ and 4.06 m) in Fig. 3. Simulated u-velocities were within 3% of the observed values at $x=2.43$ (ADP to be placed at $x=2.3$) except in the lower 5 cm of the flow (about 15% of the total depth). Comparisons of velocity profiles at $x=4.06$ m were not as good as at $x=2.43$ m, having errors ranging from approximately 1% to 20%. This larger deviation is believed to be due to the lack of homogeneity in the flow throughout the cross section that could not be represented in the

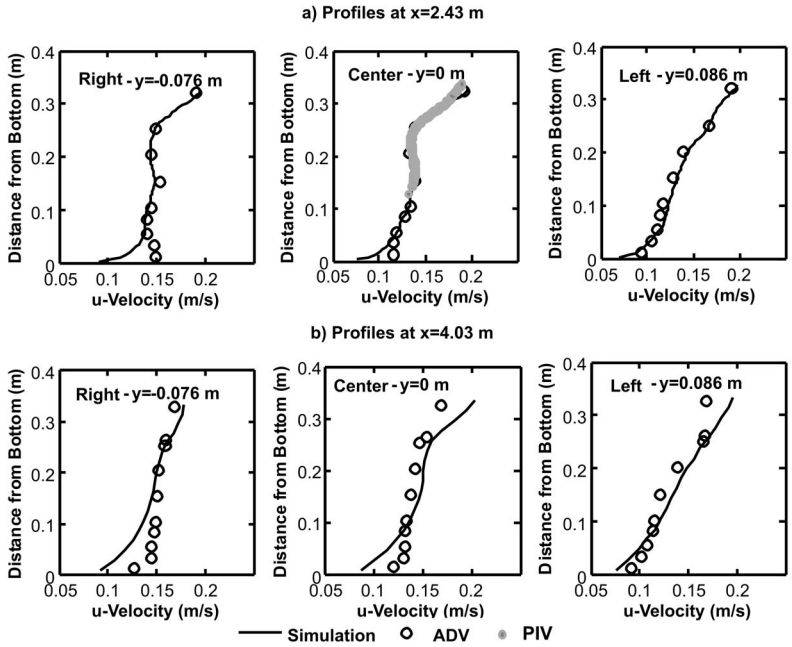

Fig. 3. Profiles of u-velocity comparing simulated to acoustic Doppler velocimeters (ADV) and particle image velocimetry (PIV) for longitudinal locations in the flume at (a) $x=2.43$ m; (b) $x=4.03$ m

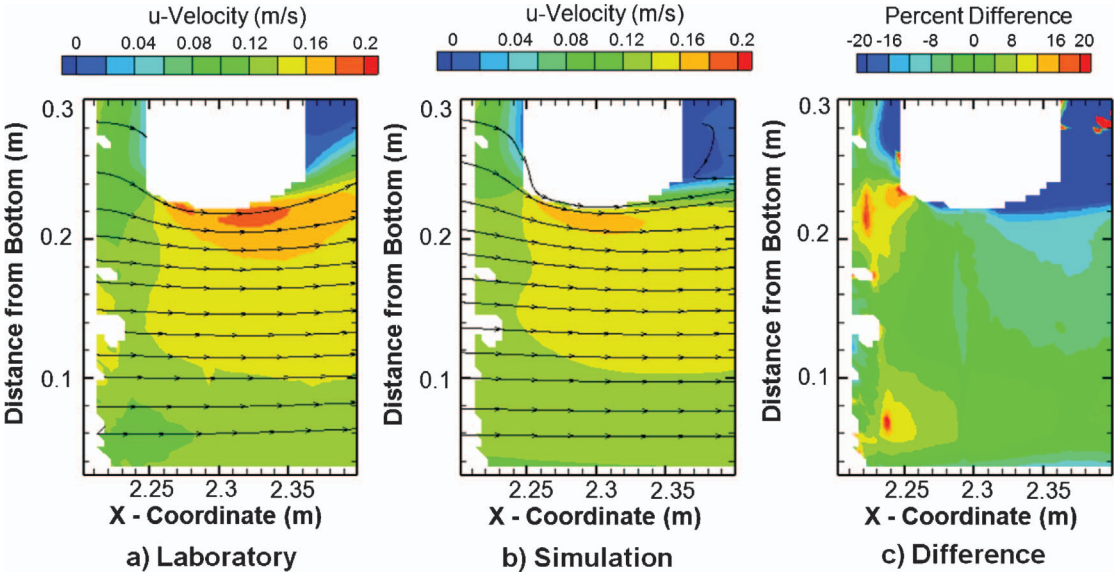

Fig. 4. (Color) *u*-velocities measured in the laboratory (a); simulated in the numerical model (b); and the percent difference (c) with the acoustic Doppler current profile deployed in the flume

CFD boundary conditions. Measurements made using an ADV and PIV on the centerline of the flume agreed well (Fig. 3).

The actual geometric shape of the ADP was included in the CFD model as a three-dimensional solid object (stereolithograph file) and properly represented in the model by the FAVOR method (Flow Science, Inc. 2005; Hirt and Sicilian 1985). The results of the simulation (Fig. 4) show both similarities and deviations from the velocities observed at the centerline of the flume. The model represented the flow field well beyond about 5 cm from the transducers, but did not compute as large of an area of acceleration adjacent to the instrument or as fast a wake recovery as were observed in the flume experiments. Given the uncertainty in the flume boundary conditions, the CFD simulations were reasonable.

Simulation of Field Measurements

The comparison of the CFD model to experimental data indicated that the CFD model was capable of modeling the flow field around an ADCP. Model simulations were conducted corresponding to the field data collected on the Delta Mendota Canal (Gartner and Ganju 2002). The field data do not contain detailed velocity measurements around the instrument, but rather the velocities that were measured by the instrument itself. Therefore, the simulated flow field was processed using a user-developed computer program to obtain the velocity profile that the ADCP would have measured from that flow field.

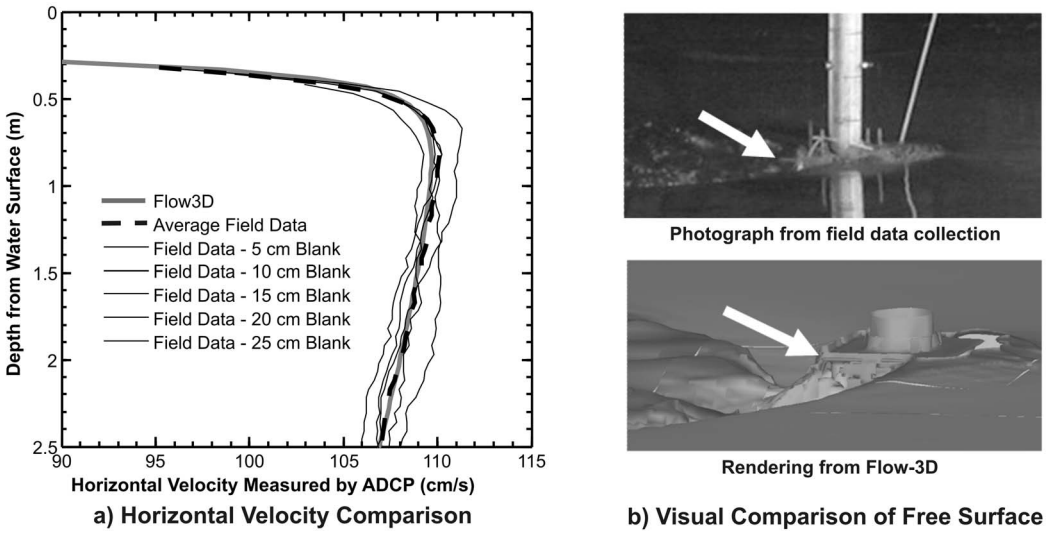

Fig. 5. Comparison of simulated and observed ADCP measured velocity profiles (a); qualitative comparison of free surface between photograph during data collection and rendering of modeled free surface (b)

Table 1. Summary of Hydraulic Characteristics

Simulation	Instrument approach velocity (m/s)	Mean velocity (m/s)	Instrument diameter (m)	Flow depth (m)	Immersion depth (m)	Flow Reynolds number	Instrument Reynolds number	Flow Froude number	Instrument Froude number
Run 1	0.39	0.35	0.1	1.5	0.14	5.23×10^5	3.89×10^4	0.09	0.33
Run 2	0.77	0.7	0.1	1.5	0.14	1.05×10^6	7.68×10^4	0.18	0.66
Run 3	1.2	1.1	0.1	1.5	0.14	1.65×10^6	1.20×10^5	0.29	1.02
Sim 1	0.36	0.34	0.2	5.4	0.215	1.81×10^6	7.18×10^4	0.05	0.25
Sim 2	1.1	1.04	0.2	5.4	0.215	5.61×10^6	2.19×10^5	0.14	0.76
Sim 3	2.2	2.10	0.2	5.4	0.215	1.13×10^7	4.39×10^5	0.29	1.51

Flow Field Simulation

Custom boundary conditions were developed for the model to allow use of a specified logarithmic velocity profile for initial and upstream boundary conditions. The parameters for the logarithmic velocity profile were determined from the unbiased velocities measured by the ADCP. Five velocity profiles were averaged to obtain a mean velocity profile [Fig. 5(a)]. The mean velocity data were assessed and only the portion of the mean velocity profile that showed increasing velocity magnitude with increasing distance from the streambed were used (4.63 to 2.69 m from the bed or a depth of 0.77 to 2.71 m). An iterative approach, assuming the roughness k_s and computing shear velocity $u*$ from linear regression, was used until the regression was optimized (coefficient of determination of 0.99). The computational mesh was created to minimize the influence of the boundary conditions on the flow field surrounding the ADCP and to ensure that the ADCP and mount were properly represented in the model by the FAVOR method. The ADCP and mount used to deploy the instrument were replicated in FLOW-3D using a combination of a stereolithograph file of the actual ADCP geometry and primitive objects created in the modeling software to represent the deployment configuration. The ends of bolts, the connector, and the ridges on the top of the ADCP were smoothed using primitive holes and objects in FLOW-3D to obtain an accurate but computationally efficient representation of the instrument and mount. Several different mesh configurations were evaluated for their ability to accurately represent the ADCP and mount geometry, and to minimize the effect of numerical solutions and boundary effects. Six nested blocks were used to model the instrument and surrounding flow. The smallest inside block around the instrument had a mesh spacing of 0.6 cm with each subsequent block doubling the mesh spacing until the outermost block had a mesh spacing of about 19.5 cm. The computational domain extended from 2.54 m upstream of the centerline of the ADCP to 1.95 m downstream and to each side of the ADCP. A flat streambed with a roughness of 1.5×10^{-6} m, determined from the regression discussed above, was located at a depth of 5.40 m below the water surface.

Computation of ADCP Velocities from a Simulated Flow Field

A comparison of the simulated results with measured field data required that the velocity the ADCP would have measured in simulated flow field be determined. Each nested block was extracted into an ASCII file containing the x, y, and z spatial coordinates and u, v, and w velocity components for the center of each computational cell. The location of the path of each beam was mapped into the computational mesh. Velocity data from the block with the finest mesh spacing available for the specific beam location were used to compute the simulated beam velocity. The acoustic beam was represented as a cylinder with a diameter of 5.1 cm tilted at an angle of 20 deg from the vertical. The cylindrical assumption is valid for the near field, defined as from the transducer to a range of 1.7 m (Steve Maier, Teledyne RD Instruments, 3/22/2005, oral communication), which is the region of primary interest for this analysis. Uniformly distributed points spaced 0.3 cm apart lying within the ellipse, formed by the tilted acoustic cylinder, were computed and the u, v, and w velocity components for each of these points were interpolated from the simulation results. The mean u, v, and w velocity components were then computed as the mean of the points inside the ellipse,

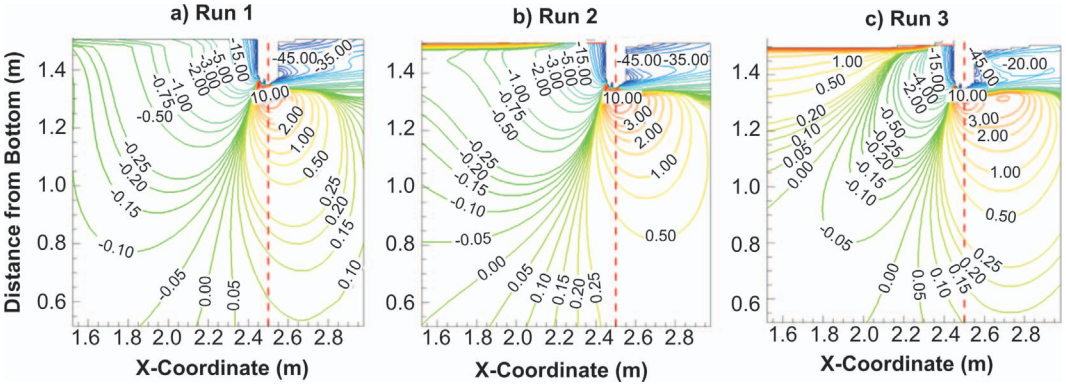

Fig. 6. (Color) Percent difference between simulated u-velocity with and without the acoustic Doppler profiler for Run 1 (a); Run 2 (b); and Run 3 (c)

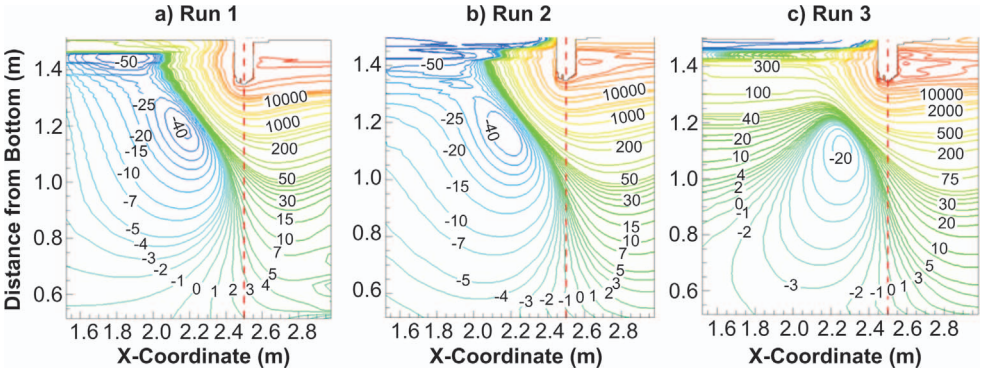

Fig. 7. (Color) Percent difference between simulated turbulent kinetic energy with and without the acoustic Doppler profiler for Run 1 (a); Run 2 (b); and Run 3 (c)

yielding a velocity for each beam at each z-coordinate in the computational mesh. Beam velocities were computed by converting the u, v, and w velocity components for each beam to the velocity component parallel to the beam. Using a standard transformation matrix (RD Instruments 1999), the beam velocities were converted to u, v, and w velocity components that would be measured by the ADCP in the simulated flow field. Finally, the velocity profile was averaged into bins matching the configuration of the ADCP using the weighted averaging procedure applied in the ADCP (RD Instruments 1996).

Discussion of Results

The ADCP velocity profile computed from the simulated flow field compared closely with the mean of the ADCP velocity profiles observed by Gartner and Ganju (2002). Simulations were run until the model had reached dynamic equilibrium. A simulated ADCP profile is plotted in Fig. 5(a) together with the five observed velocity profiles from the Delta Mendota Canal collected on January 24, 2002, and the mean of those five profiles. The CFD model simulation produced results with mean differences between the simulated and field profile of 0.1% with a coefficient of variation of 0.2% and a maximum deviation from the observed data at any point in the profile of 1%. A qualitative comparison of the free-surface condition is shown in Fig. 5(b), where part of the ADCP mount can be seen in both the photograph and the rendered surface from the CFD model. Comparison of the field data reported by Gartner and Ganju (2002) and the numerical simulations of those data confirm the hypothesis that velocities measured close to an ADCP not only violate the flow homogeneity assumption, but have magnitudes that are contrary to expected velocities near a flow obstruction. This comparison also supports use of the numerical model to study the effects of the deployment configuration, immersion depth of the instrument, and streamflow conditions on the flow disturbance and resulting ADCP velocity measurements.

Simulation of Different Velocity Fields

The CFD model was used to simulate three different velocity fields for both the Teledyne RD Instruments Rio Grande and the SonTek/YSI ADP. Two additional simulations (one at a faster velocity and one at a slower velocity) using the Delta Mendota Canal configuration were completed (Sim 1 and 3; Sim 2 is the original simulation). In addition, three model runs using the ADP in three different fully developed turbulent flow conditions were simulated in a straight channel 1.5 m deep (Runs 1, 2, and 3). The hydraulic characteristics of these simulations are shown in Table 1. The flow Reynolds and Froude numbers were computed using the depth of flow and the mean flow velocity. The instrument Reynolds number was computed using the diameter of the ADCP as the length variable and the velocity in the portion of the flow blocked by the ADCP. The instrument Froude number was computed using the immersion depth as the length variable and the velocity in the portion of the flow blocked by the ADCP.

Discussion of Dimensionless Parameters

The simulations at increasing Reynolds and Froude numbers indicate the potential importance of these dimensionless parameters

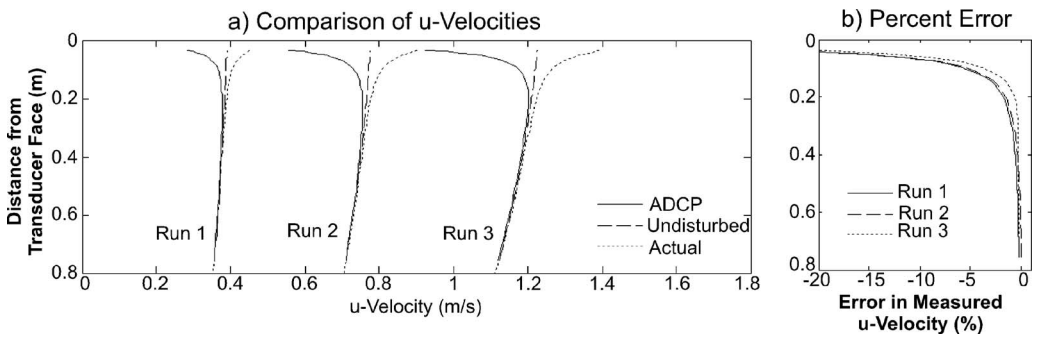

Fig. 8. Comparison of ADCP computed, undisturbed, and actual velocities (a); and the percent error in measured velocity compared with the undisturbed velocity for each different simulation (b) using the Sontek/YSI ADP

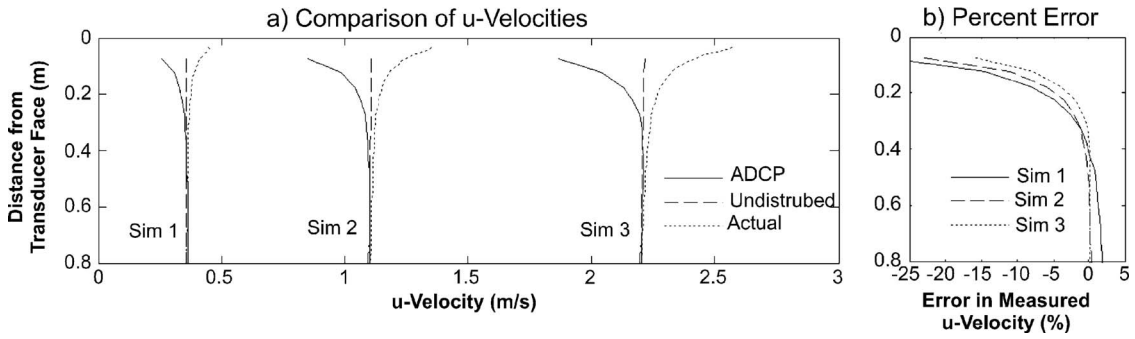

Fig. 9. Comparison of ADCP computed, undisturbed, and actual velocities (a); and the percent error in measured velocity compared with the undisturbed velocity for each different simulation (b) using the Teledyne RD Instruments Rio Grande

of the flow field around an ADCP and thus, on the error in ADCP measurements in the disturbed flow. The percent change in the u-velocity and TKE as compared to simulations with no ADP are shown in Figs. 6 and 7, respectively, for Runs 1–3. Positive and negative contours represent increases and decreases of the flow velocity and turbulent kinetic energy due to the presence of the ADP. Deceleration of the flow occurs upstream from the ADP along the water column and downstream from the probe only in the region behind it, while acceleration of the flow occurs in the region below the instrument. For high Reynolds and Froude numbers (Run 3), an upstream region with accelerated flow (Fig. 6) and high TKE (Fig. 7) was found.

The hypothesis that the ADCP measures neither the undisturbed stream velocity nor the actual velocity of the flow field near the instrument is clearly shown in Figs. 8(a) and 9(a). The magnitude of the bias in ADCP-measured velocities ranged from more than 25% at 5 cm from the transducers to less than 1% at about 50 cm from the transducers for the scenarios simulated [Figs. 8(b) and 9(b)]. Although the difference in measured velocity compared to the undisturbed velocity (no ADCP/ADP) is larger in magnitude at higher velocities, the error as a percent difference is greater and extends further into the water column at lower velocities. Research relating drag on an infinite cylinder to the cylinder Reynolds number indicates decrease in drag when the Reynolds number reaches 2×10^5 (Schlichting 1979; Roshko 1961). Run 3 and Sim 3 have instrument Reynolds numbers approaching or exceeding this threshold. In addition, Run 3 and Sim 3 have instrument Froude numbers greater than 1 for the immersion depth simulated. On the basis of these data, as undisturbed velocity increases the flow below the ADCP separates near the center of the instrument and the error in measured velocity is slightly reduced. However, as Froude number increases, the deformation of the free surface also increases upstream and downstream from the instrument (Fig. 10). These deformations are important. The shape of the obstacle (i.e., deployment configuration) could increase the free-surface deformations, which could produce entrainment of air, modification of the water column hydrodynamics, and redirection of the velocity vectors (Fig. 10). Conversely, a properly designed deployment could reduce the free-surface deformation and minimize changes in the hydrodynamics, thus improving the performance of the ADCP for near-instrument velocity measurements. Therefore, additional research is required to fully develop the relation between dimensionless parameters, shape of the deployment configuration, and the expected error in ADCP measurements.

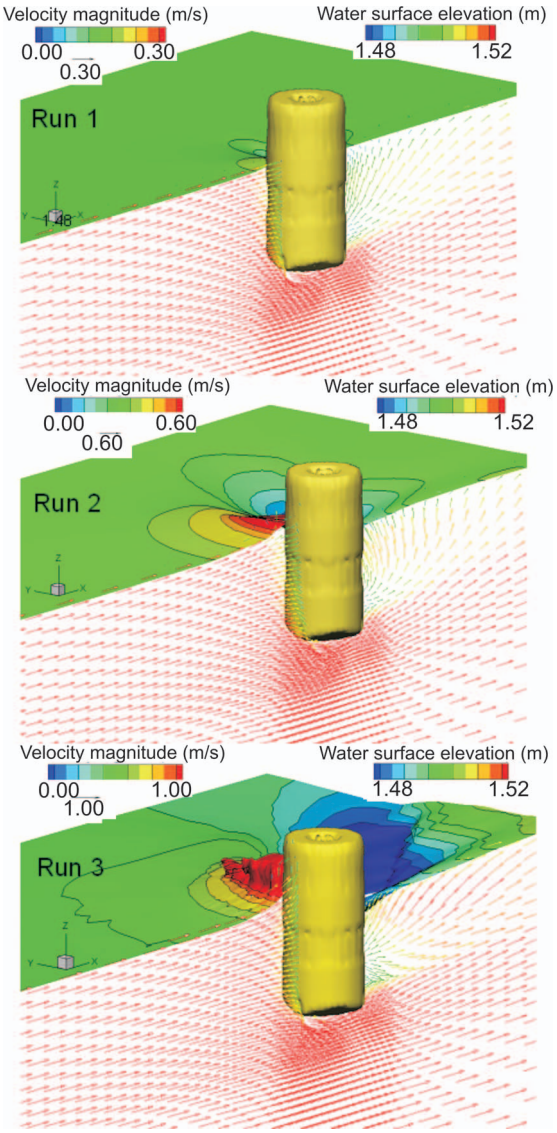

Fig. 10. (Color) Water-surface contours and velocity vectors for simulations, Runs 1, 2, and 3 of flow around a SonTek/YSI acoustic Doppler profiler

Discussion of Free-Surface and Rigid-Lid Simulations

Abad et al. (2004) reported numerical simulation results of a straight channel using the rigid-lid approximation for the free surface. Comparing the results of Abad et al. (2004) with the results obtained herein using VOF technique for the free surface shows that simulations using a rigid lid to represent the free surface overestimates the flow disturbance (velocity field) around the instrument because the rigid-lid approximation (vertical velocity equal to zero) is violated near the ADCP. Similar results were found for the case of flow around square and circular piers (Tseng et al. 2000). Although the validity of the rigid-lid assumption would depend on the Froude number and on the shape of the ADCP and deployment platform, the free-surface simulations presented herein suggest that a VOF approach is more reliable and universally applicable to a variety of conditions.

Conclusions

The results obtained from the validated numerical model simulations indicate that the ADCP modifies the flow field it is trying to measure, resulting in erroneous measurements of the mean flow velocities and turbulent quantities near the instrument. These erroneous measurements are caused by the flow pattern that develops around the ADCP, which violates the assumption of flow homogeneity required to resolve beam velocities measured by the ADCP into Cartesian velocity components. Therefore, velocity measurements close to the ADCP and in shallow-water environments where the ADCP may be a significant obstruction to flow may be biased by the flow disturbance and should be critically evaluated. The magnitude and spatial extent of the errors in measured velocities are shown to vary with instrument Reynolds and Froude numbers. However, current research is not sufficient to define a relation between dimensionless parameters and the expected error in ADCP velocity measurements. Full characterization of these effects will require additional simulations for a wide range of conditions. VOF free-surface modeling is shown to be a valid approach for evaluating the flow disturbance created by the ADCP.

Future Work

The magnitude and spatial extent of errors in velocity measurements and turbulent kinetic energy calculations for common deployment configurations in a wide range of flow conditions are needed to provide guidance on the limitations of ADCPs. In addition, design of fairings or changes in instrument shape that might minimize the effects of flow disturbance need to be investigated. The validity of the numerical simulations should continue to be evaluated using actual measurements of the flow field around the ADCP and ADCP-measured velocity profiles for different Reynolds and Froude numbers. Various turbulence closure models and their effect on modeling the unsteady motion of the flow around the ADCP due to the frequency of production and shedding of vortices on ADCP measurements should also be investigated.

Acknowledgments

The U.S Geological Survey and Environment Canada provided financial support for this work. The writers are grateful to Mariano I. Cantero for providing valuable suggestions and to Rodrigo A. Musalem and Francisco Pedocchi for their assistance with laboratory experiments.

Notation

The following symbols are used in this paper:

k_s = boundary roughness projection;
u = velocity component in x-direction;
$u*$ = shear velocity;
v = velocity component in y-direction;
w = velocity component in z-direction;
x = streamwise positional coordinate;
y = cross-stream positional coordinate; and
z = vertical positional coordinate.

References

Abad, J. D., Musalem, R. A., Garcia, C. M., Cantero, M. I., and Garcia, M. H. (2004). "Exploratory study of the influence of the wake produced by acoustic Doppler velocimeter probes on the water velocities within measurement volume." *Proc., Critical Transitions in Water and Environmental Resource Management* (CD-ROM), ASCE, Reston, Va.

Ahmed, F., and Rajaratnam, N. (1998). "Flow around bridge piers." *J. Hydraul. Eng.*, 124(3), 288–300.

Barbhuiya, A. K., and Dey, S. (2004). "Measurement of turbulent flow field at a vertical semicircular cylinder attached to the sidewall of a rectangular channel." *Flow Meas. Instrum.*, 15, 87–96.

Barkhudarov, M. R. (2004). "Multiblock gridding technique for FLOW-3D." *Flow Science technical note No. FSI-02-TN59-R2*, Flow Science, Inc., Santa Fe, N.M.

Eberhard, B., and Wille, R. (1972). "Periodic flow phenomena." *Annu. Rev. Fluid Mech.*, 4, 313–340.

Flow Science, Inc. (2005). *Flow-3d v. 9.0 user's manual*, Flow Science, Inc., Santa Fe, N.M.

Fulford, J. M. (1992). "Characteristics of U.S. Geological Survey discharge measurements for water year 1990." *Open-File Rep. 92-493*, U.S. Geological Survey, Stennis Space Center, Miss.

Gartner, J. W., and Ganju, N. K. (2002). "A preliminary evaluation of near-transducer velocities collected with low-blank acoustic Doppler current profiler." *Proc., Hydraulic Measurements and Experimental Methods* (CD-ROM), ASCE, Reston, Va.

Hirt, C. W., and Nichols, B. D. (1981). "Volume of fluid (VOF) method for the dynamics of free boundaries." *J. Comput. Phys.*, 39, 201–225.

Hirt, C. W., and Sicilian, J. M. (1985) "A porosity technique for the definition of obstacles in rectangular cell meshes." *Proc., Fourth Int. Conf. Ship Hydro.*, National Academy of Science, Washington, D.C.

Hoyt, J. W., and Sellin, R. H. J. (2000). "A comparison of the tracer and PIV results in visualizing water flow around a cylinder close to the free surface." *Exp. Fluids*, 28, 261–265.

Iliescu, T., and Fischer, P. F. (2003). "Large eddy simulation of turbulent channel flows by the rational large eddy simulation model." *Phys. Fluids*, 15(10), 3036–3047.

Jacobson, R. B., Elliott, C. M., and Johnson, H. E., III. (2004). "Assessment of shallow-water habitat availability in modified dike structures, lower Missouri River." *Open-File Rep. 2004-1409*, U.S. Geological Survey, Denver.

Johnson, K. R., and Ting, F. C. K. (2003). "Measurements of water surface profile and velocity field at a circular pier." *J. Eng. Mech.*, 129(5), 502–513.

Meneveau, C., and Katz, J. (2000). "Scale-invariance and turbulence models for large-eddy simulation." *Annu. Rev. Fluid Mech.*, 32, 1–32.

Oberg, K. A., Morlock, S. E., and Caldwell, W. S. (2005). "Quality-

assurance plan for discharge measurements using acoustic Doppler current profilers." *Scientific Investigations Rep. 2005-5183*, U.S. Geological Survey, Denver.

Oberg, K. A., and Mueller, D. S. (1994). "Recent applications of acoustic Doppler current profilers." *Proc., Fundamentals and Advancements in Hydraulic Measurements and Experimentation*, ASCE, Reston, Va., 341–350.

Pope, S. B. (2004). "Ten questions concerning the large-eddy simulation of turbulent flows." *New J. Phys.*, 6(35).

RD Instruments. (1996). *Principles of operation: A practical primer—Second edition for broadband ADCPs*, RD Instruments, San Diego, Calif.

RD Instruments. (1999). "ADCP coordinate transformation booklet: Teledyne RD Instruments." ⟨http://www.rdinstruments.com/x/cs/documents.html⟩ (March 31, 2006).

Reichl, P., Hourigan, K., and Thompson, M. C. (2005). "Flow past a cylinder close to a free surface." *J. Fluid Mech.*, 533, 269–296.

Richardson, J. E., and Panchang, V. G. (1996). "Three-dimensional simulation of scour-inducing flow at bridges piers." *J. Hydraul. Eng.*, 124(5), 530–540.

Roshko, A. (1961). "Experiments on the flow past a cylinder at very high Reynolds numbers." *J. Fluid Mech.*, 10, 345–356.

Roulund, A., Sumer, M., Fredsoe, J., and Michelsen, J. (2005). "Numerical and experimental investigation of flow and scour around a circular pile." *J. Fluid Mech.*, 534, 531–401.

Savage, B. M., and Johnson, M. C. (2001). "Flow over Ogee spillway: Physical and numerical model case study." *J. Hydraul. Eng.*, 127(8), 640–649.

Schlichting, H. (1979). *Boundary layer theory*, 7th Ed., McGraw-Hill, New York.

Sheridan, J., Lin, C., and Rockwell, D. (1997). "Flow past a cylinder close to a free surface." *J. Fluid Mech.*, 330, 1–30.

Shyy, W., Thakur, S. S., Ouyang, H., Liu, J., and Blosch, E. (1997). *Computational techniques for complex transport phenomena*, Cambridge University Press, New York.

Simpson, M. R. (2002). "Discharge measurements using a broadband acoustic Doppler current profiler." *Open-File Rep. 01-01*, U.S. Geological Survey, Sacramento, Calif.

SonTek. (2000). "The SonTek ADP—Three vs. four beams." *Sontek technical note*, November, SonTek/YSI, San Diego.

Tseng, M.-H., Yen, C.-L., and Song, C. C. S. (2000). "Computation of three-dimensional flow around square and circular piers." *Int. J. Numer. Methods Fluids*, 34(3), 207–227.

Wagner, C. R., and Mueller, D. S. (2001). "Calibration and validation of a two-dimensional hydrodynamic model of the Ohio River, Jefferson County, Kentucky." *Water-Resources Investigations Rep. 01-4091*, U.S. Geological Survey, Louisville, Ky.

Yakhot, V., and Nakayama, P. (1986). "Renormalization group analysis of turbulence. I: Basic theory." *J. Sci. Comput.*, 1, 1–51.

Yakhot, V., and Smith, L. M. (1992). "The renormalization group, the ε-extension and derivation of turbulence models." *J. Sci. Comput.*, 7, 35–61.

Younis, B. A., and Przulj, V. P. (2005). "Computation of turbulent vortex shedding." *Comput. Mech.*, 37(5), 408–425.